

Appearance of a saddle point in the energy spectrum of $\text{Bi}_{1-x}\text{Sb}_x$ alloys

S. Sh. Akhmedov, R. Herrmann, K. N. Kashirin, A. Krapf, V. Kraak, Ya. G. Ponomarev, and M. V. Subakova

S. U. Umarov Physico-Technical Institute, Tadzhik SSR Academy of Sciences

(Submitted 15 September 1989)

Zh. Eksp. Teor. Fiz. **97**, 663–680 (February 1990)

We investigate experimentally the electron Fermi surface of the semimetallic alloys $\text{Bi}_{1-x}\text{Sb}_x$ in the composition interval $0.22 < x < 0.6$. We have observed an electronic-topological transition of the kind described by I. M. Lifshits which consists of the confluence of two isolated portions of the electron isoenergetic surface, which are initially shifted with respect to the L point in opposite directions relative to the mirror symmetry plane, to form a single dumbbell-shaped Fermi surface. This topological transition is a consequence of the appearance of a saddle point in the electronic energy spectrum of the $\text{Bi}_{1-x}\text{Sb}_x$ alloys as a result of inversion of the bands about L with increasing x . We show that the transformation of the electronic Fermi surface in these alloys can be described over the entire interval of composition $0 < x < 0.6$ in terms of the McClure-Choi dispersion relation when certain of the parameters of this relation are allowed to vary with x .

INTRODUCTION

Bi and Sb are typical semimetals,¹⁻³ which form a continuous series of solid solutions $\text{Bi}_{1-x}\text{Sb}_x$, whose characteristic feature is a transition to a semiconducting phase in the concentration interval $0.07 < x < 0.22$ (Refs. 4–6). The semiconducting alloys $\text{Bi}_{1-x}\text{Sb}_x$ belong to the class of narrow-gap materials with “thermal” gaps, i.e., gaps less than 30 meV. Band structure calculations for Bi and Sb (Refs. 7 and 8) show that the reason for the transition of these alloys to the semiconducting phase is the differing symmetries of the terms which determine the top of the valence band in Bi (the term T_{45}) and in Sb (the terms in H). As the antimony concentration x increases, the top of the valence band (the term T_{45}) shifts rapidly downward along the energy axis and reaches the bottom of the conduction band (term L_a) for $x \sim 0.07$ (Ref. 6). In the process of removing the band overlap, the terms of the reduced Brillouin zone invert at the L point, leading to a transition to the gapless state for $x \approx 0.04$ (Refs. 9 and 10).

The reconstruction of the band structure in the $\text{Bi}_{1-x}\text{Sb}_x$ alloys with increasing x in the region $0 < x < 0.22$ has been quite well studied up to now.^{4-6,9-15} At the same time, data on the band structure of the alloys in the composition interval $0.22 < x < 0.75$ is clearly inadequate, although it has also been established that the semiconductor-semimetal transition at $x \approx 0.22$ comes about because of the appearance of an overlap of the conduction band at the L point with the extrema of the valence band at H .^{16,17} Thus, the symmetry of the terms which determine the top of the valence band in the semimetallic alloys $\text{Bi}_{1-x}\text{Sb}_x$ for $x > 0.22$, remains unchanged up to pure Sb ($x = 1$).^{17,18}

The electronic Fermi surface in bismuth consists of three different quasiellipsoids which are centered with respect to the L points and which are rotated out of the basal plane at an angle $\Theta = +6^\circ 21'$ (Refs. 3 and 7). The entire complex of experimental data obtained for the electrons at L is described by the McClure-Choi dispersion relation,¹⁹ which is calculated using the $\mathbf{k} \cdot \mathbf{p}$ method and which contains a large number of parameters which appear in first, second and third order of perturbation theory.

For small values of the energy E and the gap parameter

E_{gL} , the global characteristics of the electron Fermi surface can successfully be described by using the simplified McClure dispersion relation²⁰

$$(E + \frac{1}{2}E_{gL} + \frac{1}{2}\alpha_{v22}k_y^2)(E - \frac{1}{2}E_{gL} - \frac{1}{2}\alpha_{c22}k_y^2) = Q_{11}^2 k_x^2 + Q_{22}^2 k_y^2 + Q_{33}^2 k_z^2, \quad (1)$$

where Q_{ii} are matrix elements of the velocity operator which characterize the $\mathbf{k} \cdot \mathbf{p}$ interaction between the valence and conduction bands in the three principle directions; $(\alpha_{22})_{v,c}$ are the corrections to the inverse masses which take into account the way distant bands at L affect the curvature of $E(\mathbf{k})$ in the elongated direction of the isoenergetic surfaces at the valence band (V) and conduction band (C).

In the case of positive mass corrections ($\alpha_{v22}, \alpha_{c22} > 0$) (Refs. 19–22), a saddle point can appear in the spectrum (1) only for $E_{gL} < 0$. According to one of the widely-used models (that of Tikhovolskii and Mavroides; see Ref. 10), the gap parameter is negative in Bi and in the alloys $\text{Bi}_{1-x}\text{Sb}_x$ for $x < 0.04$, changing sign to positive ($E_{gL} > 0$) after an inversion of the bands in the $\text{Bi}_{1-x}\text{Sb}_x$ alloys for $x > 0.04$. It should be noted that up until the present time there have been no experimental data which indicate the existence of a saddle point in the Bi spectrum and in the $\text{Bi}_{1-x}\text{Sb}_x$ alloys with $x < 0.04$.

The model described above is widely used to analyze the existing experimental data, with the simplified McClure expression taken as the dispersion relation²⁰ [Eq. (1)]. However, it should be pointed out that there are a number of experimental results which cannot be explained within the Tikhovolskii-Mavroides model.¹⁰ The authors of Refs. 22 and 23 observed a sharp maximum in the anisotropy of the charge carrier cyclotron mass in the semiconducting $\text{Bi}_{1-x}\text{Sb}_x$ alloys with compositions in the range near $x \approx 0.15$. This effect cannot be explained within the framework of the model of Ref. 10. Another important discrepancy was observed by the authors of Ref. 24 in their investigation of spin effects in the semimetallic $\text{Bi}_{1-x}\text{Sb}_x$ alloys near the zero-gap state. It was established that in using the usual model of Ref. 10, agreement between theory and experiment can be obtained only with unreasonably large values of the

spin parameters. These authors observed that by changing the sign of the gap parameter they could use reasonable values of the spin parameters; this allowed them to propose a new model of the reconstruction of the band structure in the $\text{Bi}_{1-x}\text{Sb}_x$ alloys, according to which the gap parameter E_{gL} is positive in Bi and changes its sign to negative when the bands invert.

If the McClure dispersion law is correct^{19,20} and the α -parameters are positive^{19,21} within the framework of the new model,²⁴ then a saddle point must appear when the energy spectrum of the $\text{Bi}_{1-x}\text{Sb}_x$ alloys is inverted, and the function $E(\mathbf{k})$ must acquire a double-humped ("camel back") form in the conduction and valence bands.

In this paper, we will investigate quantum oscillations in the magnetoresistance (the Shubnikov-deHaas effect) in single-crystal samples of semimetallic $\text{Bi}_{1-x}\text{Sb}_x$ alloys in the composition interval $0.219 \leq x \leq 0.6$ at liquid-helium temperatures and in magnetic fields $0 \leq H \leq 55$ kOe, when the magnetic field is rotated in the twofold-bisector ($\mathbf{H} \perp C_3$) and bisector-trigonal ($\mathbf{H} \perp C_2$) planes. It was observed that with increasing x in the region of concentrations $0.255 < x < 0.26$ there occurs in these alloys a confluence of two separated portions of the electron Fermi surface, which are displaced from one another relative to the L point of the reduced Brillouin zone in opposite directions in the reflection symmetry plane, into a single isoenergetic surface of dumbbell form (a so-called electronic-topological or Lifshits transition).

Intraband magnetic breakdown is observed in $\text{Bi}_{1-x}\text{Sb}_x$ alloys between the two portions of the electron Fermi surface at L . Direct experimental proof has been obtained of the strongly dumbbell-like shape of the isoenergetic surface which appears after the Lifshits transformation takes place.²⁵

We have investigated the transformation of the electron energy spectrum at L in the composition interval $0 \leq x \leq 0.6$, which can be successfully described by the McClure dispersion relation²⁰ under the condition that a number of its parameters depend on x . A comparison of theory with experiment is given for concentration dependences of the cross-section of the electron Fermi surface and the cyclotron mass of the charge carriers.

MEASUREMENT METHOD; OBJECTS OF INVESTIGATION

The field dependences of the magnetoresistance $\rho(H)$ and its derivatives $\partial\rho(H)/\partial H$ and $\partial^2\rho(H)/\partial H^2$ were measured in the range of magnetic fields $0 \leq H \leq 5.5$ T for the temperatures $1.8 \leq T \leq 4.2$ K. Single-crystal samples of $\text{Bi}_{1-x}\text{Sb}_x$ alloys were placed at the center of a superconducting solenoid in a drumlike rotating apparatus. The angle of rotation of the samples relative to the direction of the magnetic field \mathbf{H} was determined to within $\pm 0.1^\circ$ by using an induction recorder included in the tracking system.

A signal proportional to $1/H$, and also a signal $\propto \pm \alpha H \pm \beta H^2$ used to cancel the monotonic variation of $\rho(H)$ or $\partial\rho(H)/\partial H$, was generated using an analog computer setup. The signal $\rho(H)$, after subtracting the signal $\rho(0)$ and the monotonic variation, was amplified by an F-118/1 photoelectric amplifier. The record of the Shubnikov oscillations in $\partial\rho(H)/\partial H$ and $\partial^2\rho(H)/\partial H^2$ was generated using the standard modulation technique. The signal proportional to $\partial\rho(H)/\partial H$ or $\partial^2\rho(H)/\partial H^2$ was passed to a narrow-band

amplifier and phase detector; the monotonic trace was subtracted out at the output of the phase detector. The record of the Shubnikov-deHaas oscillations was generated as a function of both direct and inverse magnetic field on a two-dimensional plotter.

The single-crystal $\text{Bi}_{1-x}\text{Sb}_x$ alloys were prepared by the method of zone melting. The rate of motion of the zone was chosen so as to exclude the possibility of a cellular substructure because of concentration supercooling. Determination of the concentration of these alloys was carried out by using a "CAMEBAX SX" x-ray microscopic analyzer.

Samples of rectangular shape with characteristic dimensions $0.5 \times 0.5 \times 3$ mm³ were cut along the principal crystal axes from single-crystal billets using an electron milling apparatus. An additional visual selection allows us to exclude those samples with twinned inclusions.

After the samples were etched in a polishing etch and washed in ethyl alcohol, current contacts made of 100 μm diameter copper wire were soldered to their ends with Wood's metal. The potential contacts (tinned copper wire of diameter 50 μm) were melted to the central parts of the samples at distances 0.5 mm from one another by using electric spark welding. The samples of $\text{Bi}_{1-x}\text{Sb}_x$ alloys used for the investigation in this paper are listed in Table I.

EXPERIMENTAL RESULTS

In recording the Shubnikov oscillations in the magnetoresistance $\rho(H)$ of the $\text{Bi}_{1-x}\text{Sb}_x$ alloys in the longitudinal ($\mathbf{H} \parallel \mathbf{j}$) and transverse ($\mathbf{H} \perp \mathbf{j}$) configurations, we observed all the characteristic features of oscillations which are intrinsic to pure bismuth.^{26,27} First of all, in passing from the longitudinal to the transverse configuration, the phase of the oscillations in $\rho(H)$ changes by 180° ; as successive Landau levels separate from the Fermi level, $\rho(H)$ passes through a maximum for $\mathbf{H} \perp \mathbf{j}$ and a minimum for $\mathbf{H} \parallel \mathbf{j}$. Secondly, as the temperature is lowered from 4.2 K to 1.8 K the amplitude of the oscillations in $\rho(H)$ in the transverse configuration ($\mathbf{H} \perp \mathbf{j}$) increases in the ordinary way,²⁸ while in the longitudinal configuration ($\mathbf{H} \parallel \mathbf{j}$) it decreases; this is due to the specific properties of inter-level phonon scattering at low temperatures.²⁶

Taking into account the facts described above, we note that the temperature dependence of the oscillation amplitudes in the longitudinal magnetoresistance for the $\text{Bi}_{1-x}\text{Sb}_x$ alloys under discussion cannot be used to calculate the cyclotron mass of the charge carriers using the standard methods. In this paper, the cyclotron mass of the carriers is calculated by the usual procedure,¹¹ when the angle between \mathbf{H} and \mathbf{j} is $\geq 60^\circ$, at which stage there are no anomalies.

In all the $\text{Bi}_{1-x}\text{Sb}_x$ alloy samples investigated (see Table I) quantum oscillations in the magnetoresistance $\rho(H)$ and its derivatives $\partial\rho(H)/\partial H$ and $\partial^2\rho(H)/\partial H^2$ were observed over a wide interval of angles as the magnetic field was rotated in the twofold-bisector ($\mathbf{H} \perp C_3$) and bisector-trigonal ($\mathbf{H} \perp C_2$) planes. The calculations presented in this paper showed that the concentration of electrons and holes at liquid helium temperatures vary within the following limits: $2.1 \cdot 10^{16} \text{ cm}^{-3} \leq N \leq 1.61 \cdot 10^{18} \text{ cm}^{-3}$. The free charge carriers in these alloys appear as a result of the overlap of the valence band (the terms at the H point) and the

TABLE I. Experimental and theoretical values of the quasiclassical frequencies of the SdH oscillation periods (which are proportional to the extremal cross-sections) and cyclotron masses for the semimetallic alloys $\text{Bi}_{1-x}\text{Sb}_x$ ($0.219 < x < 0.33$) for $\text{H} \parallel C_2$, and also the calculated values of the energy E . The energy gap is measured within the limits $-43 < E_{gL} < -69.9$ meV, while concentrations of carriers of both types at L were measured within the following limits: $2 \cdot 10^{-16} \text{ cm}^{-3} < N = P < 1.61 \cdot 10^{18} \text{ cm}^{-3}$.

	Compo- sition x , at. %	Energy, meV	Electron concen- tration N_L 10^{17} cm^{-3}	Quasiclassical frequency						Cyclotron mass						
				Δ_{max}^{-1} , kOe			Δ_{min}^{-1} , kOe			$m_{c, max}/m_0$			$m_{c, min}/m_0$			
				Exper.		Theor.	Exper.		Theor.	Exper.		Theor.	Exper.		Theor.	
				Neck	Bell		Neck	Bell		Neck	Bell		Neck	Bell		
1	0.219	19.0	0.21	48.7	18.7	48.7	-	1.7	-	1.34	0.042	0.087	-	0.50	-	0.60
2	0.254	25.1	1.50	66.5	56.5	56.5	-	5.5	-	5.59	-	0.123	-	-	-	0.83
3	0.255	25.8	1.70	76.0	74.4	74.4	-	6.2	-	6.05	-	0.188	-	0.59	-	0.85
4	0.260	26.5	1.95	165.5	161.7	161.7	-	6.1	0.048	6.82	-	0.310	-	0.66	0.69	0.88
5	0.261	27.2	2.20	177.0	177.3	177.3	-	6.8	0.380	7.35	0.166	0.251	-	0.81	0.71	0.90
6	0.273	31.4	4.00	256.5	256.5	256.5	-	10.2	2.130	11.1	0.185	0.218	-	0.97	0.82	1.00
7	0.286	38.7	8.40	393.0	393.0	393.0	-	18.6	7.020	19.1	0.204	0.212	-	1.37	1.00	1.28
8	0.288	41.1	10.20	437.0	437.0	437.0	-	18.0	9.405	22.03	0.220	0.213	-	-	1.09	1.35
9	0.288	40.0	9.40	418.0	417.9	417.9	-	19.0	8.140	20.84	-	0.213	-	-	1.06	1.32
10	0.330	47.2	16.10	570.0	570.2	570.2	-	31.4	11.060	32.75	-	0.228	-	1.52	1.27	1.61

conduction band (the terms at the L point). According to the model of Ref. 24, in the alloys under discussion the energy spectrum at L is taken to be inverted ($E_{gL} < 0$) with respect to the spectrum of bismuth, while the values of the gap parameter vary within the limits $-43 \text{ meV} \leq E_{gL} \leq -69.9 \text{ meV}$. In the table we also present the calculated values of the energy E for all the samples under study.

The angular dependence of the frequency of the Shubnikov-deHaas oscillations allows us to reconstruct the shape of the Fermi surface for each $\text{Bi}_{1-x}\text{Sb}_x$ alloy sample with $x > 0.22$. We also studied the angular dependence of the cyclotron mass of the charge carriers. With regard to the character of the angular dependences of the observed oscillations, it was necessary to refer them to the electron Fermi surface at the L point of the reduced Brillouin zone. In this paper we observed no oscillations from the hole Fermi surface.

In the case of an ellipsoidal Fermi surface, in the general case three independent frequencies should be observed from the three isolated portions of the electron Fermi surface as the magnetic field is rotated in the basal plane ($\mathbf{H} \perp C_3$). For ($\mathbf{H} \parallel C_2$) (where C_2 is the twofold axis), in stronger magnetic fields there is a dominant "high-frequency" oscillation from the maximum cross section of the electron Fermi surface at the L point ("heavy" electrons), while in weak magnetic fields there are "low-frequency" oscillations from near the minimum cross section, which also correspond in magnitude to the cross sections of the two other isolated surfaces at the L point ("light" electrons). These oscillations are well separated in magnetic field.

When the field direction deviates from the twofold direction C_2 , the oscillation frequencies deviate from the cross section which is close to minimum, because the low-frequency oscillations are beat notes of two frequencies. As the angle between \mathbf{H} and C_2 increases, the high-frequency oscillations shift toward the region of weak magnetic fields and creep up on the low-frequency oscillations.

A detailed analysis of the high-frequency oscillations in the $\text{Bi}_{1-x}\text{Sb}_x$ alloys with $x > 0.261$ shows that when the field direction deviates from the twofold direction the decrease in the Shubnikov oscillation frequency is anomalously rapid (compared to the $\text{Bi}_{1-x}\text{Sb}_x$ alloys with $x < 0.26$). In this case, the amplitude of the oscillations grows rapidly. These peculiarities indicate that there is an unusual anisotropy in the Fermi surface for alloys with $x \leq 0.261$.

As shown in Ref. 11, in n -type $\text{Bi}_{1-x}\text{Sb}_x$ alloys with a magnetic field \mathbf{H} beyond the quantum limit oriented near the twofold axis direction for small cross sections of the Fermi surface at L , the frequency of oscillations from the neighborhood of the maximum cross section of the isoenergetic surface can deviate strongly from its "quasiclassical" value $\Delta^{-1} = cS_p/eh$ i.e., the Lifshits-Onsager formula; here S_p is the extremal cross section of the Fermi surface in \mathbf{p} -space and Δ is the period of oscillation in inverse magnetic field ($1/H$). At the same time, in Bi and the semiconducting p -type $\text{Bi}_{1-x}\text{Sb}_x$ alloys the effect of frequency modulation of the high-frequency oscillations near the twofold axis direction is not strongly apparent due to the stabilizing action of the "heavy" holes at the Fermi surface near the T -extremum¹¹

In the alloys investigated in this paper, the decrease of the Fermi level in the ultra-quantum limit for small cross

sections can lead to an increase in the oscillation frequencies from the maximum cross section of the Fermi surface. In this paper, because of the good quality of the samples, the influence of the field-induced motion of the Fermi level on the Shubnikov oscillation frequency was successfully included. Figure 1 shows the characteristic high-frequency oscillations from the electron Fermi surface in magnetic fields both above and below the quantum-limit field for small cross sections. It is clear from the inset to Fig. 1 that the frequency modulation of the high-frequency oscillations due to the motion of the Fermi level in the magnetic field leads to only a weak distortion of the function $n(1/H)$. The disagreement between the observed frequency and the "quasiclassical" frequency (as $\mathbf{H} \rightarrow 0$) is less than 4% (at least over an interval of angles between \mathbf{H} and C_2 of 15°). This correction was included in the calculations of the extremal cross sections of the electron Fermi surface.

We have established that in $\text{Bi}_{1-x}\text{Sb}_x$ alloys with $x < 0.26$ the angular dependence of the extremal cross section is satisfactorily described by the ellipsoidal model.^{3,11,16,29} The ratio of the maximum cross section of the electron surface to the minimum cross section satisfies $S_{\max}/S_{\min} \approx 12$ and varies little within the composition interval $0.22 < x < 0.26$.

In alloys with $x > 0.26$ the character of the Shubnikov oscillations near the twofold axis direction undergoes a qualitative change. For the alloys with $x \geq 0.26$, in a narrow interval of angles $\Theta = \pm 5^\circ$ between \mathbf{H} and C_2 we observed a discontinuous doubling of the frequency (Fig. 2), which is similar to the oscillations caused by spin damping (this very interpretation was invoked in Ref. 16). In this paper we propose another explanation for the observed features, specifically that the doubling of the oscillation frequency near the twofold axis direction (Fig. 2) is caused by intraband magnetic breakdown between two isolated portions of the elec-

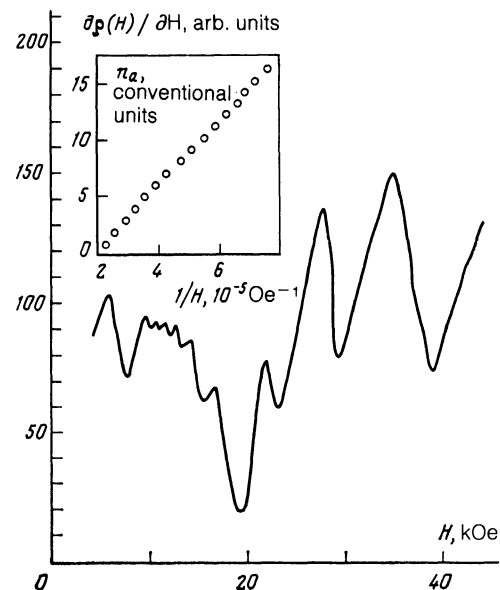


FIG. 1. Shubnikov oscillations in $\partial\rho(H)/\partial H$ from the electronic Fermi surface at L in $\text{Bi}_{1-x}\text{Sb}_x$ alloys with $x = 0.288$ in magnetic fields up to and beyond the quantum limit at $T = 2.1 \text{ K}$ and with the magnetic field rotated in the basal plane ($\mathbf{H} \perp C_3$), where the angle between \mathbf{H} and C_2 is 7.9° . The inset shows the dependence of the relative quantum number (n) on the inverse magnetic field ($1/H$).

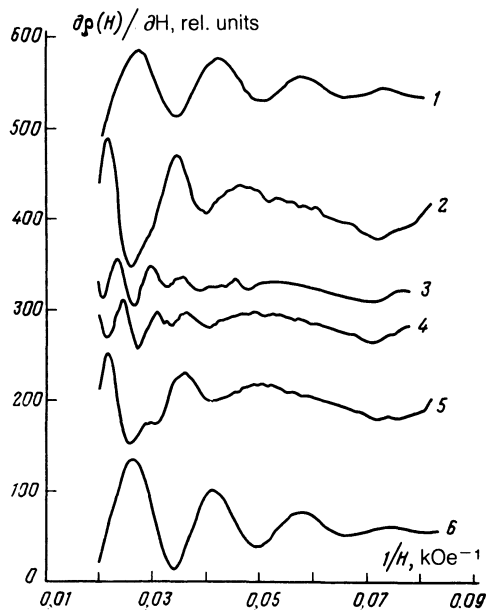


FIG. 2. Shubnikov "high-frequency" oscillations in $\partial\rho(H)/\partial H$ from the neighborhood of the maximum cross section of the electronic Fermi surface in $\text{Bi}_{1-x}\text{Sb}_x$ alloys with $x = 0.26$ at $T = 4.2$ K as a function of inverse magnetic field. The magnetic field was rotated in the basal plane ($\mathbf{H}\perp C_3$), where the angle between \mathbf{H} and C_2 was $\theta = 3.9$ (1), 1.1 (2), 0.5 (3), -0.4 (4), -1.6 (5), and -2.9 (6).

tron Fermi surface which are located in the immediate vicinity of the L -point.

Upon further increasing the composition x , we observed in those $\text{Bi}_{1-x}\text{Sb}_x$ alloys with $x > 0.26$ a sharp but monotonic frequency variation in place of the discontinuous doubling of the frequency near $\mathbf{H}\parallel C_2$. In moving off the two-fold-axis direction, the frequency of the oscillations dropped

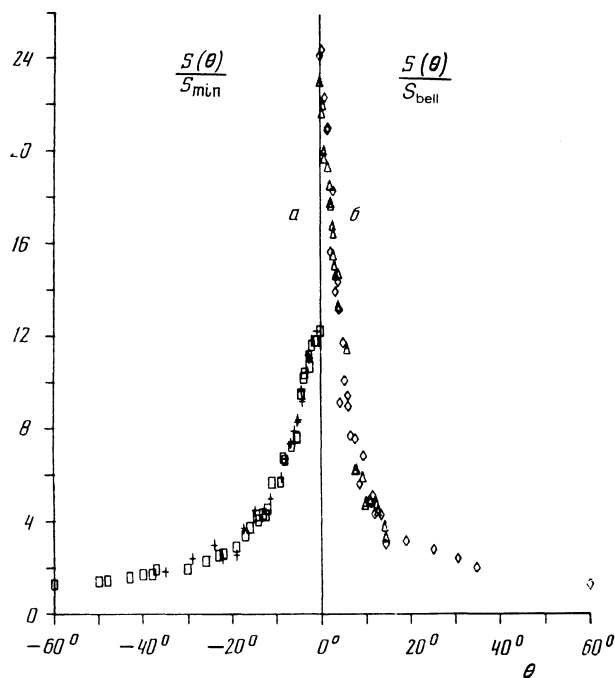


FIG. 3. Angular dependence of the reduced electron Fermi surface at L as the magnetic field is rotated in the basal plane ($\mathbf{H}\perp C_3$) for $\text{Bi}_{1-x}\text{Sb}_x$ alloys before (a) and after (b) the electronic-topological transition; + is $x = 0.219$, \square is $x = 0.255$, \triangle is $x = 0.286$, and \diamond is $x = 0.288$, ($\theta = 0^\circ$ for $\mathbf{H}\parallel C_2$).

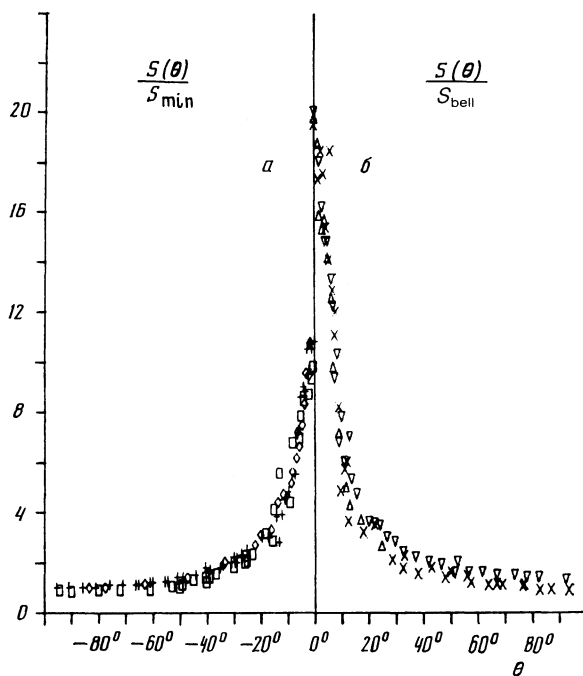


FIG. 4. Angular dependence of the reduced electron Fermi surface at L as the magnetic field is rotated in the bisector-trigonal plane ($\mathbf{H}\perp C_2$) for $\text{Bi}_{1-x}\text{Sb}_x$ alloys: \square is $x = 0.218$, + is $x = 0.254$, \diamond is $x = 0.255$, \times is $x = 0.286$, and ∇ is $x = 0.33$, ($\theta = 0^\circ$ for $\mathbf{H}\parallel z$).

off anomalously fast (compared to $\text{Bi}_{1-x}\text{Sb}_x$ alloys with $x < 0.26$), which indicates an unusually large anisotropy of the Fermi surface (Fig. 3). The latter can be a result of the confluence of two isolated parts of the Fermi surface into a single dumbbell-shaped surface. The ratio of the maximum cross section $S_{\text{max}}(\mathbf{H}\parallel C_2)$ of the newly created surface to the cross section of the "bell" of the dumbbell S_B in $\text{Bi}_{1-x}\text{Sb}_x$ alloys with $x \geq 0.26$ reaches a value $S_{\text{max}}/S_B \approx 24$ (Fig. 3b) and with further growth in the composition it varies only weakly.³⁰

In a qualitatively analogous fashion, the angular dependence of the frequency of the Shubnikov oscillations is restructured as the magnetic field is rotated into the bisector-trigonal plane ($\mathbf{H}\perp C_2$) (Fig. 4). The results presented in Figs. 3 and 4 indicate a qualitative restructuring of the topology of the electron Fermi surface in $\text{Bi}_{1-x}\text{Sb}_x$ alloys with x in the composition region $0.255 < x < 0.26$, which can be a consequence of the appearance of a saddle point in the energy spectrum.

Thus, we are dealing with an electronic-topological or Lifshits transition,²⁵ which takes place in the semimetallic $\text{Bi}_{1-x}\text{Sb}_x$ alloys as the composition varies in the region $0.255 < x < 0.26$. This transition can be classified as: 6 ellipsoidal surfaces \rightarrow 3 ellipsoidal surfaces.

In $\text{Bi}_{1-x}\text{Sb}_x$ alloys with $x = 0.288$ we have determined the angular dependence of the quasiclassical frequency of the Shubnikov oscillations associated with the neighborhood of the maximum cross section and the angular dependence of the cyclotron mass corresponding to this cross section. In order to calculate the cyclotron mass, we used the temperature dependence of the amplitude of the Shubnikov magnetoresistance oscillations $\rho(H)$ and its derivative $\partial\rho(H)/\partial H$. A calculation of the cyclotron mass correspond-

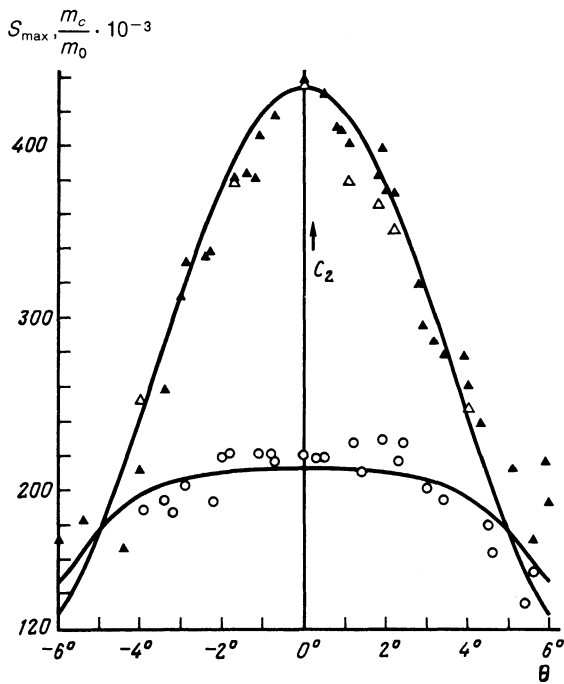


FIG. 5. Angular dependence of the reduced electron Fermi surface at L (Δ , \blacktriangle) and the cyclotron mass (\circ) near the twofold-axis direction ($\mathbf{H} \parallel C_2$ as $\theta = 0^\circ$) for $\text{Bi}_{1-x}\text{Sb}_x$ alloys with $x = 0.288$. The solid lines were plotted from the theory of Ref. 20.

ing to the maximum and close to maximum cross sections was carried out in the temperature interval 4.2 to 2.1 K as the magnetic field was rotated in the basal plane (i.e., $\mathbf{H} \perp C_3$).

When the field direction deviates from the twofold-axis direction, the quasiclassical frequency drops by almost a factor of two within a narrow angular interval $\Theta = \pm 4^\circ$ between \mathbf{H} and C_2 , while the change in the cyclotron mass is almost insignificant (Fig. 5).³¹ This fact can serve as an experimental proof of the strong dumbbell shape of the electron Fermi surface [the solid curve in Fig. 5 was plotted using the theory of McClure,²⁰ corresponding to the dispersion relation (1)].

Another experimental fact which confirms the strong dumbbell shape of the electron Fermi surface in $\text{Bi}_{1-x}\text{Sb}_x$ alloys with $x > 0.26$ is the presence of well-defined heterodyne frequencies from cross sections close to those of the "bells" and the "neck" of the dumbbell in magnetic fields below the quantum limit for small cross-sections with $\mathbf{H} \parallel C_2$. For the case of an ellipsoidal Fermi surface at the L point, for $\mathbf{H} \parallel C_2$ we should observe monochromatic oscillations from the two small cross sections which agree in size.^{6,11} As the magnetic field is rotated in the basal plane ($\mathbf{H} \perp C_3$) in the region of angles where oscillations are observed from the small cross-sections, the character of the heterodyning is quite reproducible. A Fourier analysis allows us to separate the frequencies which corresponds to the extremal central ("neck") and noncentral ("bell") cross-sections of the dumbbell-shaped Fermi surface. We observed analogous heterodyne behavior for all the remaining $\text{Bi}_{1-x}\text{Sb}_x$ alloys with $x > 0.26$.

DISCUSSION OF RESULTS

The electronic-topological Lifshits transition observed in this paper for narrow-gap semimetallic $\text{Bi}_{1-x}\text{Sb}_x$ alloys,

which consists of the confluence of two isolated portions of the electron Fermi surface into a single isoenergetic surface of dumbbell shape, is possible only in the case where a camel-back (double hump) is present in the spectrum. Thus, the results presented in this paper indicate that a saddle point is present in these $\text{Bi}_{1-x}\text{Sb}_x$ alloys.

In principle, the McClure dispersion relation²⁰ (1) allows for this possibility. When the inverse mass corrections α_{v22} and α_{c22} are positive in the elongation direction (the y -direction), the saddle point arises in the region where the spectrum is inverted ($E_{gL} < 0$) at a certain critical value of the gap parameter E_{gL}^* , and the function $E(\mathbf{k})$ acquires a camel-back form for $|E_{gL}| > |E_{gL}^*|$. The reason for this can be understood starting from the following considerations. According to data from band-structure calculations,^{7,9,21} the terms in the energy spectrum of Bi which determine the valence band and the conduction band at the L point interact strongly among themselves. There is also a weak additional interaction with four distant bands which must be included in the elongated direction of the isoenergetic surfaces. In the case of a direct ($E_{gL} > 0$) spectrum, the contributions to the curvature of the valence band and conduction band from their interaction and from interaction with the distant bands have the same sign.

A characteristic of an inverted ($E_{gL} < 0$) spectrum is the fact that the inverse masses determined by the interaction of bands located close to one another differ in sign from those due to their interactions with distant bands, both in the conduction and in the valence bands. Under certain conditions, the resulting effective mass at the bottom of the band reduces to zero, and the mass itself goes to infinity. In this case, the function $E(\mathbf{k})$ in the neighborhood of the extremal point disappears, which corresponds to the point at which the saddle point appears in the spectrum.

According to our new model,²⁴ the restructuring of the energy spectrum at the L point in $\text{Bi}_{1-x}\text{Sb}_x$ alloys is a result of the inversion of the bands at L : as x increases a transition occurs from a direct spectrum (Bi , $E_{gL} > 0$) to an inverted spectrum (i.e., the alloys with $x > 0.04$, $E_{gL} < 0$). The dependence of the gap parameter E_{gL} on x is described by the expression (see Ref. 29)

$$E_{gL} = (10 - 242x) \text{ meV.} \quad (2)$$

Equation (2) is used in this paper to calculate the value of E_{gL} in the alloys under study.

Note that we have not set ourselves the task of determining the value of the gap parameter E_{gL} from the intrinsic experimental data, since a large number papers^{6,10,12,13} exist where the absolute value of the gap parameter is determined quite reliably (see Fig. 6).

As we have already noted earlier, the appearance of the saddle point in the electronic energy spectrum in $\text{Bi}_{1-x}\text{Sb}_x$ alloys, and also all the existing experimental data collected up to now on these alloys, can be described consistently within the framework of the simple McClure dispersion relation (1).²⁰ In this case, the best agreement between theory and experiment is attained by making a number of the parameters entering into Eq. (1) x -dependent:

$$Q_{11} = 0.457 - 0.188x, \quad (3)$$

$$Q_{22} = 0.03 - 0.04x, \quad (4)$$

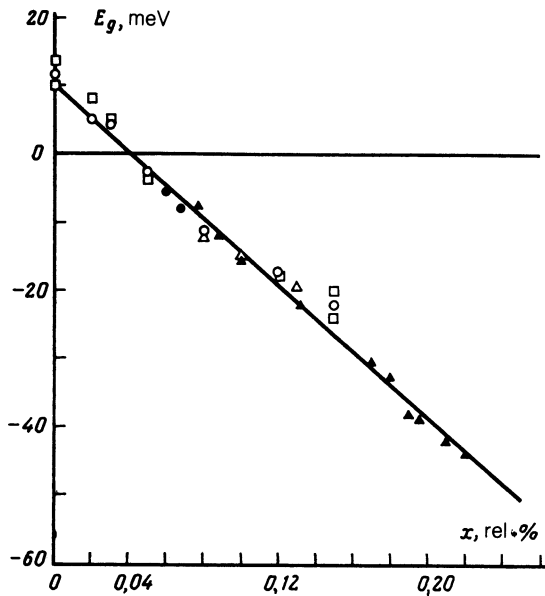


FIG. 6. Concentration dependence of the gap parameter in L for $\text{Bi}_{1-x}\text{Sb}_x$ alloys; \square is from Ref. 5, \circ is from Ref. 10, \bullet is from Ref. 12, \triangle is from Ref. 13, and \blacktriangle is from Ref. 22.

$$Q_{33} = 0.344, \quad (5)$$

$$\alpha_{v22} = 1.1 + 0.7x, \quad (6)$$

$$\alpha_{c22} = 0.615 + 0.4x. \quad (7)$$

The Fermi energy of electrons in the semimetallic $\text{Bi}_{1-x}\text{Sb}_x$ alloys for $x > 0.22$, as measured from the center of the gap at L , is given by the relation

$$E = (47.5 + 287.1x) \text{ meV}, \quad (8)$$

which is valid at least in the composition interval $0.22 < x < 0.6$.

Results of calculations of the function $E(k)$ in the neighborhood of the L point in the direction of elongation (the y -direction) calculated on the basis of the dispersion relation (1), within the framework of the new model²⁴ with the parameters (2)–(8), are shown in Fig. 7. It follows from these calculations that the saddle point in the conduction band appears at $x = 0.15$, and the one in the valence band at $x = 0.18$. For semiconducting $\text{Bi}_{1-x}\text{Sb}_x$ alloys in the composition range $0.22 < x < 0.26$ the Fermi level drops into the conduction band, which leads to the filling of six "pockets" shifted in k -space relative to the three equivalent L points by a distance which depends on the composition x .

The volume of the six electronic Fermi surfaces located in the neighborhood of the L -points increases monotonically with increasing x . The evolution of the electronic isoenergetic contours near the bottom of the conduction band ($E = E_F$) is illustrated in Fig. 8 for $\text{Bi}_{1-x}\text{Sb}_x$ alloys with various values of x . For $x \approx 0.26$, when the Fermi level reaches the saddle point in the conduction band, the six isolated electronic surfaces merge in pairs into three dumbbell-shaped Fermi surfaces centered relative to the L points.

Note that the McClure dispersion relation²⁰ is approximate, and obviously cannot be used to describe the electron energy spectrum in antimony, where the volume of the isoenergetic surface exceeds by two orders of magnitude the

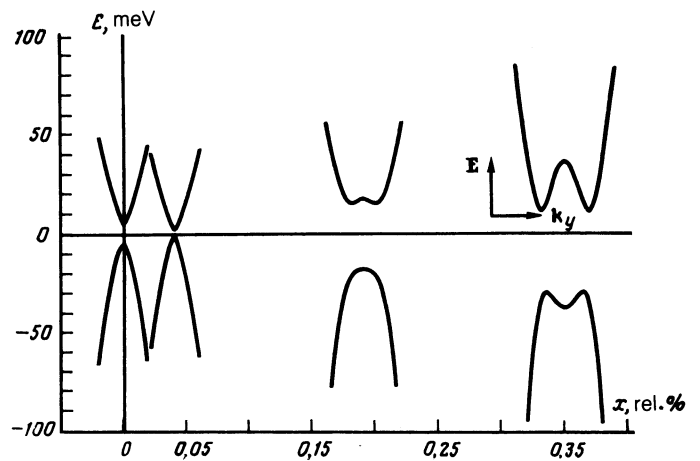


FIG. 7. Process of energy spectrum reconstruction for $\text{Bi}_{1-x}\text{Sb}_x$ alloys ($0 < x < 0.4$) at L . The calculations were carried out within the framework of the dispersion relation from Ref. 20, assuming the validity of the model in Ref. 24.

corresponding volume in bismuth ($N = P = 5 \cdot 10^{19} \text{ cm}^{-3}$ in Sb at $T = 4.2 \text{ K}$). Nevertheless, in the composition interval $0 < x < 0.6$, we can use the dispersion relation (1) to calculate with reasonable accuracy the basic charge carrier parameters at the L -point for $\text{Bi}_{1-x}\text{Sb}_x$ alloys.

The anisotropy of the isoenergetic surface as a function of x is shown in Fig. 9, where the light points denote the values of the ratio $S_{\text{max}}/S_{\text{bell}}$ calculated using our model for the dumbbell-shaped Fermi surface in the $\text{Bi}_{1-x}\text{Sb}_x$ alloys with $x \geq 0.26$, while the dark points denote values of the ratio $S_{\text{max}}/S_{\text{min}}$ in the semimetallic alloys with $0.22 < x < 0.26$ at the Fermi level and in the semiconducting $\text{Bi}_{1-x}\text{Sb}_x$ alloys ($0.07 < x < 0.22$) at the bottom of the band^{22,23} (at the bottom of the band, the anisotropy of the extremal cross section of the Fermi surface coincides quite accurately with the cyclotron mass). Let us recall that after the appearance of the saddle point at the L -point the bottom of the band is a pair of

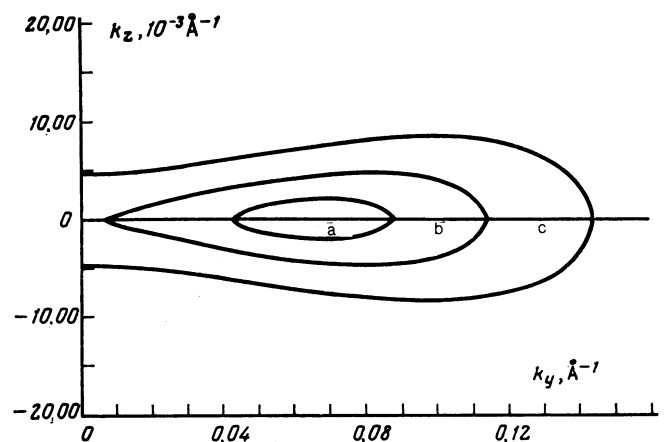


FIG. 8. Isoenergetic contours of the electron Fermi surface for $\text{Bi}_{1-x}\text{Sb}_x$ alloys as the composition varies for various energies: a—20 meV, $x = 0.23$; b—30 meV, $x = 0.25$; c—41 meV, $x = 0.3$. The calculations were carried out in terms of the simplified McClure dispersion relation from Ref. 20, assuming the validity of the model in Ref. 24.

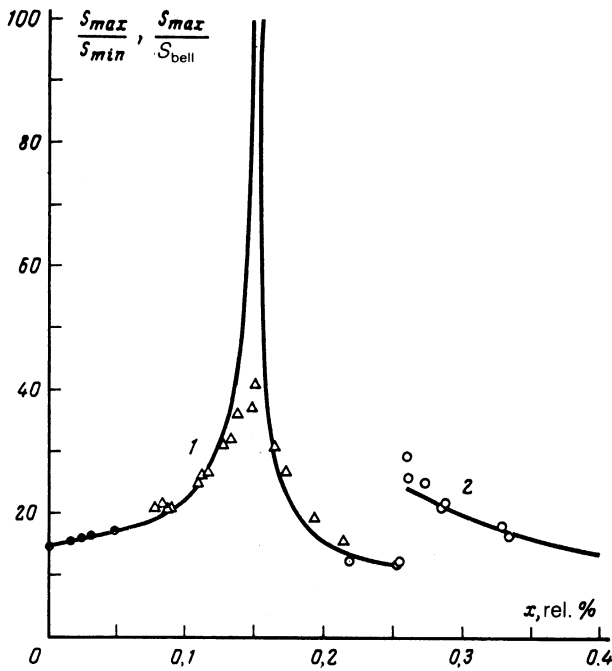


FIG. 9. Theoretical (solid trace) and experimental (symbols) concentration dependences of the ratio S_{\max}/S_{\min} (1) and S_{\max}/S_{bell} (2), which characterizes the anisotropy of the electronic Fermi surface for $\text{Bi}_{1-x}\text{Sb}_x$ alloys; ● is from Refs. 6, 11; Δ is Ref. 22, 23; ○ is from this paper.

local minima shifted with respect to the L -point in opposite directions (Fig. 7). The solid traces in Fig. 9 are derived from theory. The sharp growth in the anisotropy near $x = 0.15$ is explained by the simplification of the function $E(\mathbf{k})$ at the bottom of the band when it acquires the characteristic camel-back spectrum. The experimental results of

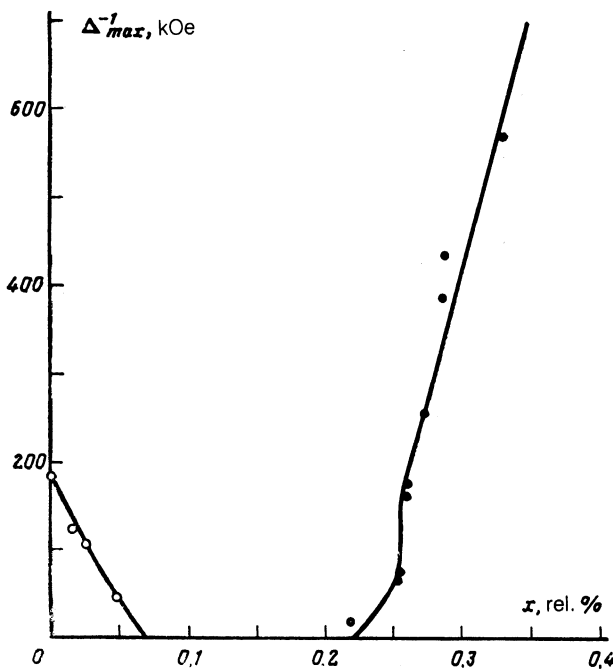


FIG. 10. Composition dependence of the oscillation frequency Δ_{\max}^{-1} on the maximum cross section of the electronic Fermi surface at L for $\text{Bi}_{1-x}\text{Sb}_x$ alloys with $\mathbf{H} \parallel C_2$; ○ is from Ref. 12, Δ is from Ref. 16, and ● is from this paper.

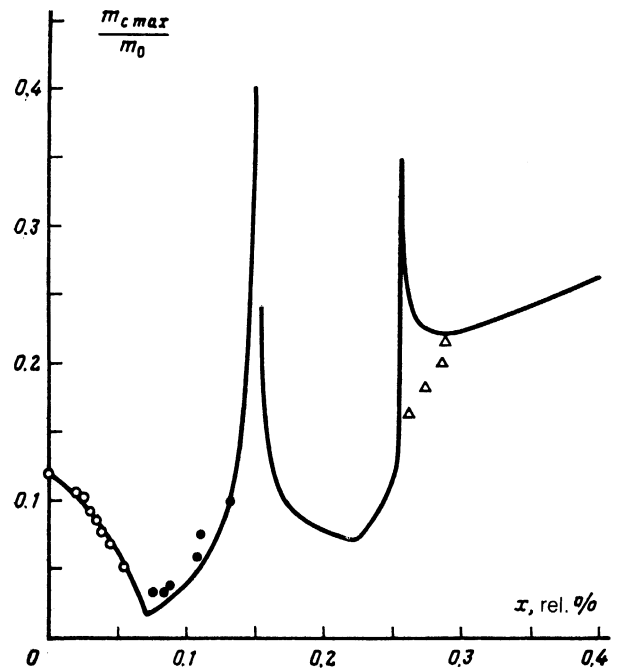


FIG. 11. Composition dependence of the cyclotron mass $m_{c,\max}$ on the maximum cross section of the electronic Fermi surface at L for $\text{Bi}_{1-x}\text{Sb}_x$ alloys (in the semiconducting phase, the masses are given for the bottom of the conduction band); ○ is from Ref. 11; ● is from Ref. 22, and Δ is from Ref. 16 and this paper.

Refs. 22 and 23 obtained for the compositions $0.07 \leq x \leq 0.22$ are in excellent agreement with the theoretical curve in Fig. 9.

It must be specially emphasized that neither the jump in the anisotropy observed in this paper at $x \approx 0.26$ nor the maximum in the anisotropy of the Fermi surface for the bottom of the conduction band for $x \approx 0.15$ (Fig. 9), can be explained in the framework of the older model of Ref. 10.

Comparison of the experimental values of the extremal cross sections of the Fermi surface and the cyclotron masses of the charge carriers in the $\text{Bi}_{1-x}\text{Sb}_x$ alloys over a wide interval of compositions (including the region of the direct spectrum $E_{g,L} > 0$ for $x < 0.04$) with theoretical calculations obtained within the framework of dispersion relation (1) of Ref. 20, assuming the validity of the new model of the reconstructed energy spectrum,²⁴ allows us to clarify the following features of this reconstruction (Figs. 10–13).

As x increases within the initial interval $0 \leq x \leq 0.07$, the values of the maximum extremal cross section decrease rapidly to zero as we pass to the semiconducting phase (Fig. 10). For alloys with $x > 0.22$ the maximal cross section of the electron Fermi surface grows with increasing x ; at $x \approx 0.26$ the cross section discontinuously doubles as a result of the electronic-topological transition. The experimental values of the quasiclassical frequency Δ_{\max}^{-1} in the semimetallic $\text{Bi}_{1-x}\text{Sb}_x$ alloys (Fig. 10) for the composition region $0.22 \leq x \leq 0.26$ pertain to the maximum cross section of pairs of "quasiellipsoids" shifted with respect to the L -point in opposite directions, while for $x \geq 0.26$ they pertain to the maximum central cross section of the dumbbell-shaped Fermi surface.

The concentration dependence of the maximum cyclotron mass $M_{c,\max}(x)$ is shown in Fig. 11. The decrease in the

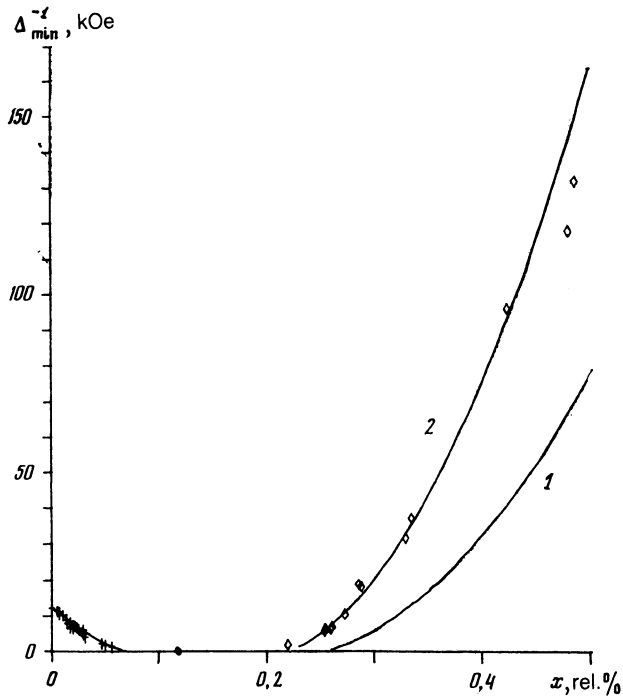


FIG. 12. Composition dependence of the Shubnikov oscillation frequency on the minimum central cross-section $\Delta_{\max, N-1}^{-1}$ (1) and the noncentral cross section $\Delta_{\max, B-1}^{-1}$ of the electronic Fermi surface at the point L for $\text{Bi}_{1-x}\text{Sb}_x$ alloys; + is from Refs. 2, 12, 14, 32, and 33; Δ is Refs. 16, 31, and this paper.

value of $M_{c, \max}(x)$ within the initial composition interval during the transition to the semiconducting phase is connected with the decrease in the Fermi energy. In the concentration region $x \approx 0.15$ a sharp growth is observed in the

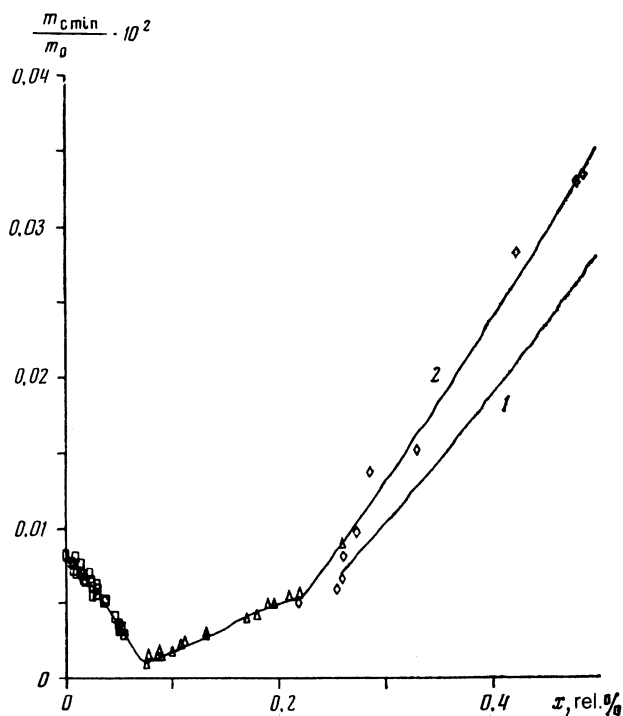


FIG. 13. Composition dependence of the cyclotron mass on the minimum central cross section $m_{c, \min, N}$ (1) and the minimum noncentral cross section $m_{c, \min, B}$ (2) of the electronic Fermi surface at L for $\text{Bi}_{1-x}\text{Sb}_x$ alloys (in the semiconducting phase, the masses are given for the bottom of the conduction band); \square is from Ref. 11, Δ is from Refs. 22, 23; and \diamond is from Ref. 16 and this paper.

maximum cyclotron mass at the bottom of the band, which is connected with the appearance of the saddle point in the spectra of the $\text{Bi}_{1-x}\text{Sb}_x$ alloys (the bottom of the conduction band flattens out at the extremum point). In the "pure" semiconducting alloys, after the appearance of the camelback spectrum (for $x \approx 0.15$), the two equivalent absolute minima in the conduction band descend in energy below the value $E = E_{gL}/2$, the charge carriers overflow into the bottom of the newly formed "pockets," and the cyclotron mass rapidly decreases with increasing x . A second sharp growth of the maximal cyclotron mass occurs as the Fermi level approaches the saddle point in the energy spectrum of the $\text{Bi}_{1-x}\text{Sb}_x$ alloys at $x \approx 0.26$. At that point, when the two isolated portions of the electronic Fermi surface coalesce, in k -space the L point becomes conical, which sends the cyclotron mass to infinity. In the real situation, magnetic breakdown most likely excludes the possibility of reaching the point with $k = 0$, and experimentally a second sharp maximum is not observed.

Figures 12 and 13 show the x -dependences of the oscillation frequencies of the minimum cross section of the electron Fermi surface δ_{\min}^{-1} and the minimum cyclotron mass $m_{c, \min}$, respectively. Also noteworthy is the presence in the semimetallic $\text{Bi}_{1-x}\text{Sb}_x$ alloys with $x > 0.26$ (for $\mathbf{H} \parallel y$) of two branches corresponding to extremal central and non-central cross sections of the dumbbell-shaped electronic Fermi surface, which form as a result of the electronic-topological transition. The experimental values of the minimum frequency and minimum cyclotron mass lie on the branches corresponding to the "bells" ($\Delta_{\min, B-1}$ in Fig. 12 and $M_{c, \min, B}$ in Fig. 13).

Let us recall that the solid traces in Figs. 5–13 were obtained based on the simplified dispersion relation (1) of Ref. 20, assuming the validity of the new model of the band structure reconstruction²⁴ and under the condition that a number of the parameters of the model of Ref. 20 [see (2)–(8)] depend on the composition of the alloy x .

In conclusion, we note that the dumbbell shape of the electron Fermi surface of the $\text{Bi}_{1-x}\text{Sb}_x$ alloys with $x \approx 0.15$ at the corresponding concentrations of charge carriers must be included in the analysis of the classical galvanomagnetic effects (i.e., the magnetoresistance and Hall effect in weak magnetic fields). In particular, the value of the Hall factor can turn out to differ considerably from unity even at liquid-helium temperatures.

We use this opportunity to express our sincere gratitude to N. B. Brandt and L. A. Fal'kovskii for useful discussions.

¹ L. A. Fal'kovskii, Usp. Fiz. Nauk **94**, 3 (1968) [Sov. Phys. Usp. **11**, 1 (1968)].

² M. S. Dresselhaus, J. Phys. Chem. Solids **32**, Suppl. p. 3 (1971).

³ V. S. Edel'man, Usp. Fiz. Nauk **123**, 257 (1977) [Sov. Phys. Usp. **20**, 819 (1977)].

⁴ F. A. Buot, J. Phys. Chem. Solids **32**, Suppl. p. 99 (1971).

⁵ G. Oelgard, G. Schneider, W. Kraak, and R. Herrmann, Phys. Status Solidi (b) **74**, K75 (1976).

⁶ G. A. Mironova, M. V. Subakova, and Ya. G. Ponomarev, Fiz. Tverd. Tela **22**, 3628 (1980) [Sov. Phys. Solid State (Leningrad) **22**, 2124 (1980)].

⁷ S. Golin, Phys. Rev. **166**, 643 (1968).

⁸ P. J. Lin and L. M. Falicov, Phys. Rev. **141**, 562 (1966).

- ⁹E. J. Tichovolski and J. G. Mavroides, *Solid State Commun.* **7**, 927 (1969).
- ¹⁰E. J. Tichovolski and J. G. Mavroides, *Sol. St. Comm.* **7**, 927 (1969).
- ¹¹G. A. Mironova, M. V. Subakova, and Ya. G. Ponomarev, *Zh. Eksp. Teor. Fiz.* **78**, 1830 (1980) [*Sov. Phys. JETP* **51**, 918 (1980)].
- ¹²B. A. Akimov, V. V. Moshchalkov, and S.M.Chudinov, *Fiz. Nizk. Temp.* **4**, 60 (1978) [*Sov. J. Low Temp. Phys.* **4**, 30 (1978)].
- ¹³G. Oelgard and R. Herrmann, *Phys. Status Solidi (b)* **75**, 189 (1978).
- ¹⁴W. Braune, G. Kuka, S. Hess *et al.*, *Phys. Status Solidi (b)* **79**, 501 (1977).
- ¹⁵W. Braune, G. Kuka, H. -J. Gollnest, and R. Herrmann, *Phys. Status Solidi (b)* **89**, 95 (1978).
- ¹⁶N. B. Brandt, R. Herrmann, and G. I. Golysheva, *Zh. Eksp. Teor. Fiz.* **83**, 2152 (1982) [*Sov. Phys. JETP* **56**, 1247 (1982)].
- ¹⁷D. V. Gitsu, F. M. Muntyanu, and M. I. Onu, *Fiz. Nizk. Temp.* **3**, 1149 (1977) [*Sov. J. Low Temp. Phys.* **3**, 557 (1977)].
- ¹⁸L. R. Windmiller, *Phys. Rev.* **149**, 472 (1966).
- ¹⁹J. W. McClure and K. N. Choi, *Solid State Commun.* **21**, 1015 (1977).
- ²⁰J. W. McClure, *J. Low Temp. Phys.* **25**, 527 (1976).
- ²¹V. A. Dorofeev and L. A. Fal'kovskii, *Zh. Eksp. Teor. Fiz.* **87**, 2202 (1984) [*Sov. Phys. JETP* **60**, 1273 (1984)].
- ²²B. Fellmuth, H. Kruger, R. Rudolph, and R. Herrmann, *Phys. Status Solidi (b)* **106**, 561 (1981).
- ²³W. Braune, B. Fellmuth, N. Kubicki, and R. Herrmann, *Phys. Status Solidi (b)* **110**, 549 (1982).
- ²⁴Ya. G. Ponomarev and M. V. Subakova, *Narrow-Gap Semiconductors and Semimetals: Abstracts from the VIIth All-Union Symposium*. Lvov, 1986, Part 2, p. 164.
- ²⁵I. M. Lifshits, *Zh. Eksp. Teor. Fiz.* **38**, 1569 (1960) [*Sov. Phys. JETP* **11**, 1130 (1960)].
- ²⁶S. Tanuma and R. Inada, *Tech. Report of ISSR (Japan)*. Series A, No. 658 (1974).
- ²⁷R. D. Brown, *Phys. Rev. B* **2**, 928 (1970).
- ²⁸R. Roth and P. N. Argyres, *Semiconductors and Semimetals*. New York: Academic Press, 1966, Vol. 1, p. 159.
- ²⁹S. Sh. Akhmedov, K. N. Kashirin, G. A. Mironova *et al.*, *VINITI Pat.* No. 8735-B87, 15 Dec. 1987.
- ³⁰N. B. Brandt, G. I. Golysheva, Nguyen Minh Thu, *et al.*, *Fiz. Nizk. Temp.* **13**, 1209 (1987) [*Sov. J. Low Temp. Phys.* **13**, 683 (1987)].
- ³¹S. Sh. Akhmedov, K. N. Kashirin, M. V. Subakova, and Ya. G. Ponomarev, *Bull. Tadzhik SSR Acad. Sci.* XXXI, 241 (1988).
- ³²N. B. Brandt, L. S. Lyubutina, and N. A. Kryukova, *Zh. Eksp. Teor. Fiz.* **53**, 134 (1967) [*Sov. Phys. JETP* **26**, 93 (1967)].
- ³³M. R. Ellet, R. B. Horst, L. R. Williams, and K. F. Cuff, *J. Phys. Soc. Jpn.* **21**, Suppl. p. 666 (1966).

Translated by Frank J. Crowne